Mathematics of aging: diseases of the posterior segment of the eye

J. A. Ferreira * Paula de Oliveira † P. M. da Silva‡ R. Silva §

Abstract

The changes caused by aging affect all body tissues. The vitreous humor, which fills the space between the lens and the retina, progressively liquefies and shrinks, eventually causing a posterior vitreous detachment. Retinal disorders caused by the breakdown of the blood retinal barrier are also associated with physiological aging. In this work a mathematical model of the pharmacokinetics of a drug eluted from an intravitreal biodegradable implant in an aging eye is presented. The influences of vitreous liquefaction and retina diseases are analyzed. The model is represented by a set of P.D.E's describing the evolution of the concentration in a drug eluting implant, coupled with two systems of partial differential equations, describing the transport of drug in the vitreous chamber and the retina. Different scenarios of the physiology of vitreous and of inflammation's degrees of the retina are numerically compared. The numerical results suggest a dominating influence of retina permeability.

Keywords: Partial Differential Equations, Numerical Analysis, Pharmacokinetics of a drug in the vitreous

1 Introduction

Delivery of drugs to the retina remains a crucial challenge because retinal disorders are major causes of irreversible vision loss, leading to blindness. In diseases of the posterior segment of the eye, intraocular drug delivery systems represent an election treatment because eye drops and systemic administration cannot deliver drug continuously and for long periods of time into the vitreoretinal tissue. Systems clinically successful are based on intraocular

*CMUC-Department of Mathematics, University of Coimbra. E-mail:ferreira@mat.uc.pt.

†CMUC-Department of Mathematics, University of Coimbra. E-mail:poliveir@mat.uc.pt.

‡Instituto Politécnico de Coimbra, ISEC, DFM, Rua Pedro Nunes, 3030-199 Coimbra, Portugal. CMUC. E-mail:pascals@isec.pt.

§Faculty of Medicine, University of Coimbra, Portugal (FMUC); Department of Ophthalmology, Centro Hospitalar e Universitário de Coimbra, Portugal (CHUC); Association for Innovation and Biomedical Research on Light and Image, Coimbra, Portugal (AIBILI). E-mail:rufino.silva@oftalmologia.co.pt.

injections and non-biodegradable or biodegradable implants, loaded with drug, which are currently used as slow release devices, delivering locally drug for extended periods of time ([11]). The influence of age-related changes on the distribution of drugs after intravitreal administration is an area of active research, from the medical and computational viewpoints. We mention, without being exhaustive the works [17], [20], [15] and [10]. In this paper we present a mathematical model that describes the pharmacokinetics of a drug delivered by an intravitreal biodegradable implant in unhealthy situations: liquefaction of the vitreous and inflammation of the retina (Figure 1).

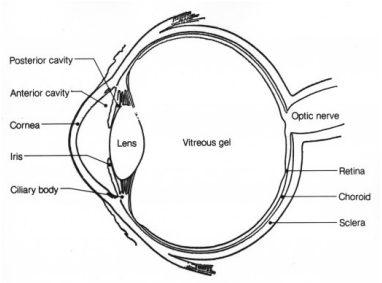

Figure 1: Anatomy of the eye ($http://usercontent1.hubimg.com$).

The vitreous humor is a clear gel that occupies the posterior compartment of the eye, between the lens and the retina (Figure 1). It maintains the shape of the eye, supplies it with nutrition and helps with the focusing of light. The vitreous humor is composed of 99% water by weight, and the other 1% is made up of special substances - collagen and hyaluronic acid-which give the vitreous its gel-like consistency. Drug molecules migrate from the polymeric biodegradable implant, inserted in the vitreous, to the retina. The distribution of drug depends on multiple factors as the properties of the release medium, that is the vitreous humor, the type and severity of retinal disorders, the physicochemical properties of the drug and the characteristics of the polymer. The purpose of our work is to study, from a mathematical point of view, how such disease conditions, influence the pharmacokinetics of a drug.

Normally, the back surface of the vitreous is in direct contact with the retina. With aging the vitreous gel exhibits a heterogeneous structure characterized by a space dependent permeability. It becomes more fluid, undergoing syneresis and forming liquid pockets called lacunae (Figure 2). The progressive liquefaction of the vitreous leads to lacunae coalescence which is normally followed by a decreasing in the adhesion of the vitreous with the retina. The separation of the posterior hyaloid face from the retina can then occur: first partially and then totally. This separation is called a Posterior Vitreous Detachment (PVD). The case of PVD is not addressed in the present paper.

In the case of vitreous liquefaction, the question then arises: can eye disease conditions, as liquefaction and retina inflammation, alter the pharmacokinetics of the drug? This raises

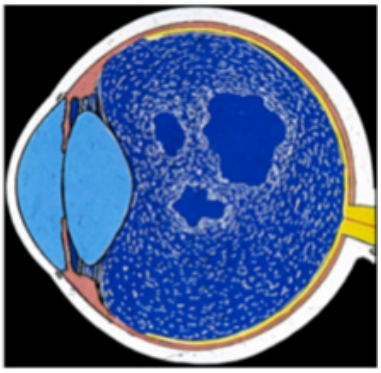

Figure 2: With aging vitreous humor forms liquid pockets called lacunae (*http* : *//retinaspecialists.com.au/wp − content/uploads/*2013/04/*new*10.*jpg*).

concern in the medical community about the drug delivery trend, namely the concentration peak and the residence time, in the case of aging conditions.

At the best of our knowledge no solid conclusions have been established until now regarding the effect of liquefaction on drug distribution. Without being exhaustive we mention two papers, where experimental results are presented, leading to different conclusions. In [8] the authors conclude, in a experimental study with Dutch-belted rabbits, that the pharmacokinetics of the drug is not altered in a vitrectomized eye, that is an eye where the vitreous humor was replaced by a substitute. On the contrary in [26] the authors, while studying drug diffusion in a liquefied vitreous, conclude that meaningful differences are observed. These two papers address the pharmacokinetics in slightly different situations: in [8] vitrectomized eyes are considered; in [26] the conclusions are established for a liquefied vitreous. However if differences are observed in a liquefied vitreous, we could expect analogous differences in a vitrectomized eye. In fact in this case the vitreous gel is replaced by a saline solution, which is progressively substituted by aqueous humor during the time.

Concerning the degree of inflammation of the retina we believe that its influence in the residence time and peak concentration has not been mathematically modeled. Mathematical models represent an invaluable tool for this study because different degrees of inflammation can be simulated, and guide *in vivo* experiments.

In vivo experiments often use juvenile animal models with no alterations in the vitreous structure, as liquefactions or retinal diseases. Some researchers have raised concerns [26] that the results of these experiments can overestimate drug efficacy. A better understanding of the impact of aging conditions is necessary to develop more effective therapies so that drug concentration is maintained within the therapeutic window at the target site for the desired period of time. Mathematical models that simulate real physiological conditions can be of great help in guiding laboratory experiments and providing outcomes for future implant development. The novelty of our approach lies in modelling two aspects of the physiological

aging of the eye: liquefaction of the vitreous and breakdown of Blood Retinal Barrier (BRB).

In previous papers, by some of the authors ([2], [13]), the pharmacokinetics of a drug released from a biodegradable implant was studied in the case of a homogeneous healthy vitreous. The transport of drug, released by an intravitreal injection, in a homogeneous completely attached vitreous has been considered in [18].

These last years there has been a certain controversy regarding the type of mechanisms underlying the transport of a drug in a healthy vitreous and in a liquefying vitreous with or without a detachment. One of the explanations is based on the substantial reduction of viscosity in a liquefied vitreous humor, which could lead to an increase in effective diffusion of a drug ([23]). The authors of paper [25] claim that the diffusion coefficients of different molecules (small and large molecular weight) measured in saline solutions or vitreous gel are similar. Their alternative explanation for a possible change in the rate at which molecules could be redistributed in a liquefied vitreous is based in a change in convection and not an increase in diffusion rates ([6]).

Following this last approach we consider that the driving phenomena involved in controlled drug delivery from a biodegradable implant, through the vitreous chamber, are diffusion, convection and polymeric degradation. Convection arises due to a flow driven by a pressure gradient between the anterior hyaloid membrane and the posterior retina surface, that is the Retinal Pigment Epithelium (RPE). In the model presented in this paper ocular globe motion is not considered. This means that the model describes more accurately the pharmacokinetics of a drug for a patient in rest, performing smooth pursuit eye movements and during the non rapid eye movement of sleep.

The mathematical model presented in this paper is represented by a set of coupled systems of partial differential equations describing the transport of drug in the implant, the vitreous humor, liquefied or non liquefied, and the retina (Figure 3). We analyze the influence of the physiological conditions that characterize a liquefying vitreous and a retinal inflammation and we establish a number of conclusions regarding their influence on residence time and concentration peaks.

In Section 2 we present the geometry and the coupled model that describes the evolution of drug concentration in the implant, the vitreous and the retina. A mass balance of the total mass drug is also established. In Section 3 we study the dependence of the pharmacokinetics on the liquefaction of the vitreous (Section 3.1) and the degree of inflammation of the retina (Section 3.2). Regarding the influence of liquefaction on drug distribution we study its direct influence on velocity and the possible occurrence of a movement of the implant. Regarding the effect of retinal inflammation we model the breakdown of the BRB. In Section 3.2 a successful treatment is also simulated. Finally in Section 4 we present some conclusions.

2 Mathematical model

2.1 Geometry of the model

The vitreous chamber is represented in Figure 3 by Ω_2. In normal conditions it is filled by vitreous humor and it occupies about two-thirds of the eye. The lens, also called crystalline lens, acts to focus images in the retina. It is modeled in Figure 3 as an ellipsoid. The anterior hyaloid membrane and the lens separate the anterior chamber and the posterior chamber of the eye from the vitreous chamber. The retina, Ω_3, forms the boundary of the vitreous chamber on the posterior surface and is modeled as the volume between two spherical surfaces with radius differing of 11 mm. We assume that the retina is a porous tissue with external boundary, which is called the Retinal Pigment Epithelium, represented by $\partial\Omega_{out}$. In this boundary the pressure results from two opposite pressures: the hydrostatic pressure and the oncotic pressure. In the interface that represents the hyaloid membrane, $\partial\Omega_{in}$, acts the intraocular pressure(IOP), that is the fluid pressure inside the eye. The rationale behind the value assigned to the pressure in $\partial\Omega_{out}$ is explained later in this paper. This pressure gradient is responsible for the convection flow between the anterior part of the vitreous chamber and its posterior part.

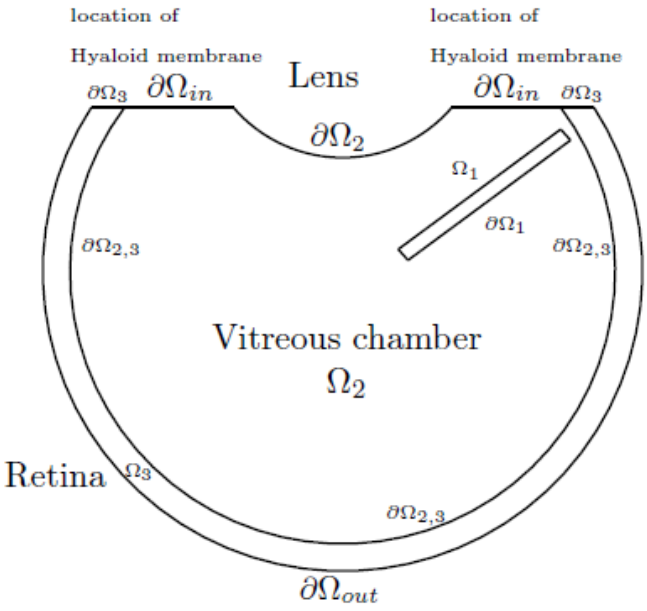

Figure 3: Geometry of the posterior segment of the eye: the implant, Ω_1, the vitreous humor, Ω_2, and the retina, Ω_3.

In Figure 3 we represent the geometry of the model. To treat diseases of the posterior segment of the eye one of the gold standard treatments is controlled release from an intravitreal

implant, Ω_1, that can be biodegradable or non biodegradable[1]. In the model presented in this paper the implant is considered biodegradable. This intravitreal implant, containing dispersed drug, is placed in the vitreous near the retina (Figure 3). It is geometrically represented by a cylinder with radius 0.023 mm and height 0.6 mm. The drug is released in a controlled manner into the vitreous which is a porous media, and its target is the retina, affected by an inflammatory process.

The geometrical model described in this section has been partially presented by the authors in [13]. However the problems studied in the present paper - liquefaction of the vitreous, clearance of the retina - have not been addressed in the previous work. Also in this paper the transport in the retina is described by a convection-diffusion equation where the convection rate is defined by Darcy's law. This modeling difference - a pure diffusive transport of drug in the retina ([13]) and a convection-diffusion transport in the present paper - leads to a more realistic description of the behavior of drug concentration in the retina.

2.2 Equations of the model

An initial amount of drug is dispersed in the polymeric implant Ω_1. We suppose that when in contact with the vitreous humor an instantaneous swelling of the implant occurs. The drug then dissolves and is transported through the implant, the vitreous chamber and the retina.

The model results from the coupling of a set of systems of partial differential equations, each one representing the transport of drug in those regions.

Transport in the implant Ω_1

Assuming that only transport by diffusion takes place in the biodegradable polymeric implant, the concentration of drug, C_1, and the molecular weight, M, of the biodegradable polymer are described by

$$\begin{cases} \dfrac{\partial C_1}{\partial t} = \nabla \cdot (D_1(M)\nabla C_1) \ \texttt{in} \ \Omega_1 \times (0,T], \\ \\ \dfrac{\partial M}{\partial t} + \beta_1 M = -\beta_2 C_1 \ \texttt{in} \ \Omega_1 \times (0,T], \end{cases} \tag{1}$$

where $D1$ stands for the diffusion coefficient of the drug in the polymeric implant, depending on M. The parameters β_1, β_2 are physical constants that characterize the degradation properties of the material. We note that the second equation in (1) is a linearized version of equation (2) used in [22]. To simplify the model we assume in this paper that the implant presents bulk degradation. In bulk degradation, no significant change occurs in the physical

[1]At present both types of intravitreal implants - biodegradable and no biodegradable - are commercialized by pharmaceutical companies.

size of the polymer carrier until it is almost fully degraded. The polymer will disappear by the end of the drug delivery process. At this point as the concentration is residual it is expected that the physical presence of the polymeric structure will have no meaningful influence in the plots. It is expected that as the polymer erodes, the molecular weight M decreases and the diffusion coefficient of the drug increases. To describe this behavior we define

$$D_1(M) = D_0 e^{\overline{k}\frac{M_0 - M}{M_0}}, \tag{2}$$

where D_0 is the diffusion coefficient of the drug in the non hydrolyzed polymer, $\overline{k}$ is a positive constant and M_0 is the initial molecular weight of the polymeric matrix ([2], [13], [22]). As $M_0 > M$ we have $D_1(M) > D_0$.

Transport in the vitreous humor Ω_2

The aqueous humor flow through the vitreous chamber has been a controversial topic for many years. Nowadays it is commonly accepted that there is a movement of aqueous humor in the vitreous chamber. The vitreous humor has a porous structure and the drug is transported by diffusion, with a coefficient D_2, and by convection with a velocity $\mathbf{v}_2$ induced by the difference of pressure, p_2, between the hyaloid membrane ($\partial\Omega_{in}$) and the interface $\partial\Omega_{2,3}$ between the vitreous and the retina. The behavior of the concentration is described by the equations

$$\frac{\partial C_2}{\partial t} + \nabla \cdot (C_2 \mathbf{v}_2) - \nabla \cdot (D_2 \nabla C_2) = 0 \,\texttt{in}\, \Omega_2 \times (0, T], \tag{3}$$

and

$$\begin{cases} \mathbf{v}_2 = -\dfrac{K}{\mu_1} \nabla p_2 \,\texttt{in}\, \Omega_2 \times (0, T] \\ \nabla \cdot \mathbf{v}_2 = 0 \,\texttt{in}\, \Omega_2 \times (0, T] \end{cases}. \tag{4}$$

In equation (3) C_2 represents the concentration of the drug in the vitreous humor, D_2 is the diffusion coefficient of the drug in the fluid (aqueous humor and liquefied vitreous gel) contained in the vitreous and $\mathbf{v}_2$ is the permeation velocity of aqueous humor given by Darcy's system (4). In this last system K denotes the permeability of the vitreous and μ_1 represents the viscosity of the permeating aqueous humour ([18]).

Transport in the retina Ω_3

The target organ, for the drug released from the intravitreal implant, is the retina. The behavior of the drug concentration in the retina is simulated considering the following equations

$$\frac{\partial C_3}{\partial t} + \nabla \cdot (C_3 \mathbf{v}_3) - \nabla \cdot (D_2 \nabla C_3) = 0 \,\texttt{in}\, \Omega_3 \times (0, T], \tag{5}$$

and

$$\begin{cases} \mathbf{v}_3 = -\dfrac{K_r}{\mu_r}\nabla p_3 \ \texttt{in}\ \Omega_3 \times (0,T] \\ \nabla \cdot \mathbf{v}_3 = 0 \ \texttt{in}\ \Omega_3 \times (0,T] \end{cases} . \tag{6}$$

In equation (5) C_3 represents the concentration of drug in the retina Ω_3 and $\mathbf{v}_3$ is the velocity of fluid permeation given by Darcy's system (6). In this last system K_r represents the permeability of the retina, μ_r the viscosity of the fluid and $\frac{K_r}{\mu_r}$ is the hydraulic conductivity of the retina ([18]).

We note that the diffusion coefficient of the drug is represented by D_2 in Ω_i, $i = 2, 3$, because it is assumed that the drug diffuses in the fluid that circulates in these regions. We recall that this fluid is composed by aqueous humor and liquefied vitreous gel. This modelling choice is based on [6]. However the properties of the transport are different in these domains because the convection rate is different: the permeability and pressure are different in Ω_2 and Ω_3.

To complete the model, initial, boundary and interface conditions are added.

Initial conditions

Initial conditions for the concentrations account for the fact that at $t = 0$ the concentration of drug is zero everywhere except in the implant, that is

$$\begin{cases} C_1(0) = C_0 \ \texttt{in}\ \Omega_1, \\ C_2(0) = 0 \ \texttt{in}\ \Omega_2, \\ C_3(0) = 0 \ \texttt{in}\ \Omega_3. \end{cases} \tag{7}$$

Boundary conditions and interface conditions

- Conditions on the pressure on $\partial\Omega_{in}$ and $\partial\Omega_{out}$ and the interfaces must be defined.

  The flow of fluid from the vitreous across the retina and Blood Retinal Barrier (BRB) results from a pressure gradient. A detailed description can be found for example in [12] and [21]. This pressure gradient is a consequence of hydrostatic forces and oncotic forces.

  On $\partial\Omega_{in}$, the anterior part of the hyaloid membrane, we consider $p = 2000Pa$. This value corresponds to a normal intraocular pressure. In Section 3.2 we illustrate the influence of intraocular pressure on drug distribution in the retina.

  In normal conditions hydrostatic and oncotic forces drive the fluid towards the choroid. These pressures combine as to produce a net vitreous-to-choroid fluid vector that tends to maintain retinal apposition. An inward movement of the fluid from the choroid into the vitreous could lead to separation of the retina from the Retinal Pigment Epithelium (RPE). A Posterior Vitreous Detachment (PVD) could then occur ([14]). Following

[21] we will assume that for a normal adult the fluid pressure on $\partial\Omega_{out}$ is $1200Pa$. The influence of this pressure on drug concentration in the retina is illustrated in Section 3.2.

It is assumed that the pressure is continuous in $\partial\Omega_{2,3}$.

- For the velocity: $\mathbf{v}\cdot\eta = 0$ on the boundaries $\partial\Omega_1$, $\partial\Omega_2$, $\partial\Omega_3$ (Figure 3). In this last equation $\mathbf{v}$ and η represent the velocity and the unit exterior normal to each one of those boundaries, respectively.

- Interface conditions for the fluxes of drug defined by $J_1 = -D_1(M)\nabla C_1$, $J_2 = -D_2\nabla C_2 + \mathbf{v}_2 C_2$, $J_3 = -D_2\nabla C_3 + \mathbf{v}_3 C_3$.

  Implant - Vitreous: $J_1\cdot\eta = J_2\cdot\eta, \quad J_1\cdot\eta = A_1(C_1 - C_2)$ on $\partial\Omega_1\times(0,T]$, where A_1 is partition coefficient of the interface implant-vitreous and η is the unit exterior normal to Ω_1 on $\partial\Omega_1$.

  The vitreous humor occupies the vitreous chamber Ω_2. Interface condition between the vitreous and the retina are considered:

  Vitreous - Retina: $J_2\cdot\eta = J_3\cdot\eta, \quad J_2\cdot\eta = A_2(C_2 - C_3)$ on $\partial\Omega_{2,3}\times(0,T]$ and $v_2\cdot\eta = v_3\cdot\eta$, where A_2 is a partition coefficient of the interface vitreous-retina and η is the unit exterior normal to Ω_2 on $\partial\Omega_{2,3}$.

As the retina is a permeable membrane, it is assumed that $J_3\cdot\eta = A_3C_3$, where η is the unit outward normal to Ω_3 on $\partial\Omega_{out}$ and A_3 is the retinal clearance. This condition means that the flux is proportional to a concentration gradient,where the drug's concentration is assumed to be null in the choroid because it is washed out very quickly. On the contrary, as the lens and the hyaloid membrane are not permeable to the drug, it is assumed that $J_2\cdot\eta = 0$ on $\partial\Omega_2\times(0,T]$, and $J_3\cdot\eta = 0$ on $\partial\Omega_3\times(0,T]$, where η is the unit outward normal to Ω_2 on $\partial\Omega_2\cup\partial\Omega_3$.

2.3 Mass conservation

The total mass of drug in the system is represented by

$$M(t) = \sum_{i=1}^{3}\int\int_{\Omega_i} C_i(x,y,t)dxdy.$$

Taking the time derivative in the last equation we have from equations (1)-(6)

$$\frac{dM}{dt}(t) = -\sum_{i=1}^{3}\int\int_{\Omega_i}\nabla\cdot J_i dxdy, \tag{8}$$

where the mass fluxes J_i are defined in the previous section. Considering the following identities

$$\begin{aligned}
\int\int_{\Omega_1} \nabla \cdot J_1 dxdy &= \int_{\partial\Omega_1} J_1.\eta ds, \\
\int\int_{\Omega_2} \nabla \cdot J_2 dxdy &= \int_{\partial\Omega_1} J_2.\eta ds + \int_{\partial\Omega_{2,3}} J_2.\eta ds + \int_{\partial\Omega_{in}} J_2.\eta ds + \int_{\partial\Omega_2} J_2.\eta ds, \\
\int\int_{\Omega_3} \nabla \cdot J_3 dxdy &= \int_{\partial\Omega_{2,3}} J_3.\eta ds + \int_{\partial\Omega_{out}} J_3.\eta ds + \int_{\partial\Omega_4} J_3.\eta ds,
\end{aligned} \tag{9}$$

and the interfaces and boundary conditions defined before, we obtain from equations (8) and (9)

$$\frac{dM}{dt}(t) = -\int_{\partial\Omega_{out}} A_3 C_3(x,y,t) dS.$$

From the last equation, we conclude that the total mass of drug in the system is a decreasing function and it is proportional to the partition coefficient of the external boundary of the retina, represented by A_3. This constant governs the clearance of the retina.

3 Numerical Simulations

In this section we analyze the behavior of drug concentration in the vitreous humor and in the retina and its dependence on different physiological factors as the liquefaction of the vitreous and the clearance by the retina. Particular attention is devoted to the residence time and the concentration peak.

The main phenomena governing the transport are diffusion in the implant Ω_1 and convection-diffusion in the vitreous chamber Ω_2 and in the retina Ω_3. The convection rates are defined by Darcy's law. In Section 3.1 an initial stage of vitreous liquefaction, represented by the existence of higher permeability zones, is addressed. In Section 3.2 the influence of pathologic clearance mechanisms of the blood-retinal barriers are studied.

The models presented are bidimensional and the geometry represents a cross section of the vitreous chamber that contains the implant. The numerical results are obtained with *COMSOL Multiphysics* version 4.2, using a piecewise finite element method, linear for the velocity and the pressure and quadratic for the concentrations. A triangulation automatically generated is used with 19862 elements. To integrate in time, adaptive Backward Differentiation Formulae, with orders between 1 and 2 and adaptive time step are used.

The numerical simulations are obtained with $C_0 = 1.7887 \times 10^3$ (mol/m^3) and $M_0 = 10^3$ $(Dalton)$, which represent the initial drug concentration and the initial molecular weight in the implant, respectively. All the media are considered isotropic. The diffusion of the drug in the implant is defined by equation (2) considering $D_0 = 10^{-13}$ (m^2/s); its diffusion coefficient in the vitreous humor is defined by $D_2 = 5.556 \times 10^{-10}$ (m^2/s). We recall that the

diffusion coefficient in the polymer will increase as the molecular weight decreases, that is as degradation occurs. The value for the diffusion coefficient is within the interval referred in the literature for Dexamethasone.

The following values of the parameters have been considered in the simulations: $K = 8.4 \times 10^{-14}\ (m^2)$, $\mu_1 = 10^{-3}\ (Pa.s)$, $\rho = 10^3\ (kg/m^3)$ and $\frac{K_r}{\mu_r} = 10^{-10}\ (m^2/(Pa.s))$. These values of the parameters have been gathered from the literature ([18]).

The values of the remaining parameters (β_1, β_2, $\overline{k}$, A_1, A_2, A_3) can not be directly measured by experiments. In this moment complete data, concerning in vivo concentrations, is not available in the literature. Consequently we don't have enough information to fit our model to experimental data. In this section we consider $\beta_1 = 10^{-7}\ (1/s)$, $\beta_2 = 10^{-10}\ (Dam^3/(mol.s))$, $\overline{k} = 1$, $A_1 = 5 \times 10^{-11}$, $A_2 = A_3 = 10^{-9}\,(m/s)$. Numerical experiments concerning the dependence on the parameters that characterize the implant (β_1, β_2, A_1, $\overline{k}$ and D) have been presented in [2] and [3]. Some numerical experiments concerning the dependence on the parameters characterizing the inflammation of the retina (A_2 and A_3) are presented in Section 3.2.

3.1 Liquefaction of the vitreous humor

In this section the effect on drug distribution of an early liquefaction of the vitreous is simulated. A normal IOP and a normal fluid pressure in the choroid have been assumed in this section.

Steady pressure and velocity for a healthy vitreous

We begin by computing the steady pressure and velocities in the vitreous humor and in the retina in healthy conditions of the vitreous, that is when no liquefaction occurs. In Figure 4 a plot of the pressure distribution is exhibited. We observe that in the vitreous chamber the pressure is almost constant, varying in the interval [1990, 2000]. We recall that 2000 Pa is the pressure on $\partial\Omega_{in}$ corresponding to a normal intraocular pressure. On the contrary there is a significant variation in the retina, [1200, 1990]. The value 1200 Pa is the fluid pressure assigned to the outlet boundary of the retina, $\partial\Omega_{out}$, that represents the Retinal Pigment Epithelium, and it corresponds to a normal fluid pressure in the choroid as explained in Section 2.

In a previous paper of the authors [13] a different pattern of the pressure was obtained. This is due to the fact that different modelling assumptions were considered. Namely a normal fluid pressure in the choroid of 1200 Pa was defined on $\partial\Omega_{2,3}$, and not in $\partial\Omega_{out}$ (Figure 3), because only diffusion was taken into account in the retina. As a consequence in [13] the interval of variation of the pressure in the vitreous chamber was [1200, 2000]. The modelling assumptions of the present paper are more realistic, because both diffusion and convection phenomena are considered ([1]).

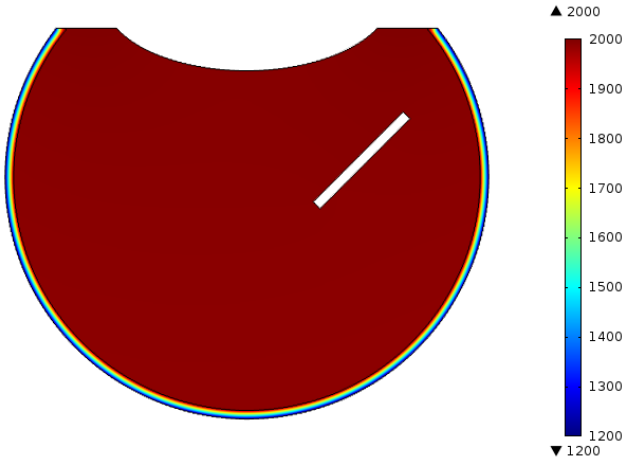

Figure 4: Steady state pressure in the vitreous and in the retina.

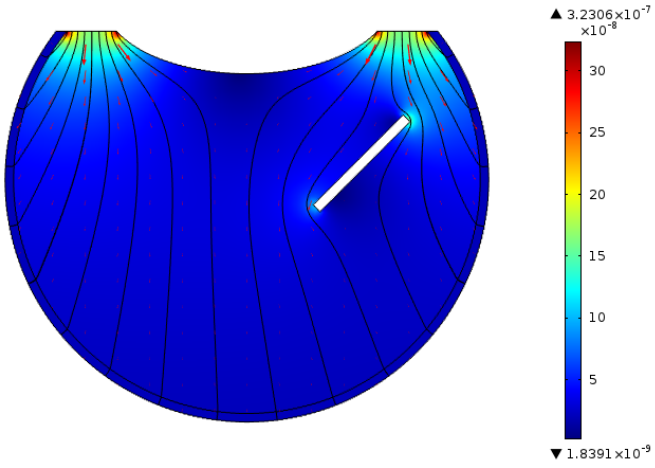

Figure 5: Steady state velocity in the vitreous and in the retina.

The velocity field computed using Darcy's law in the vitreous chamber and in the retina is presented in Figure 5. The highest values are observed in the inlet boundary, $\partial\Omega_{in}$, where the aqueous humor enters the vitreous chamber. The mean velocity is of order $10^{-8}\, m/s$. This value is in agreement with values found in the literature ([1], [18]).

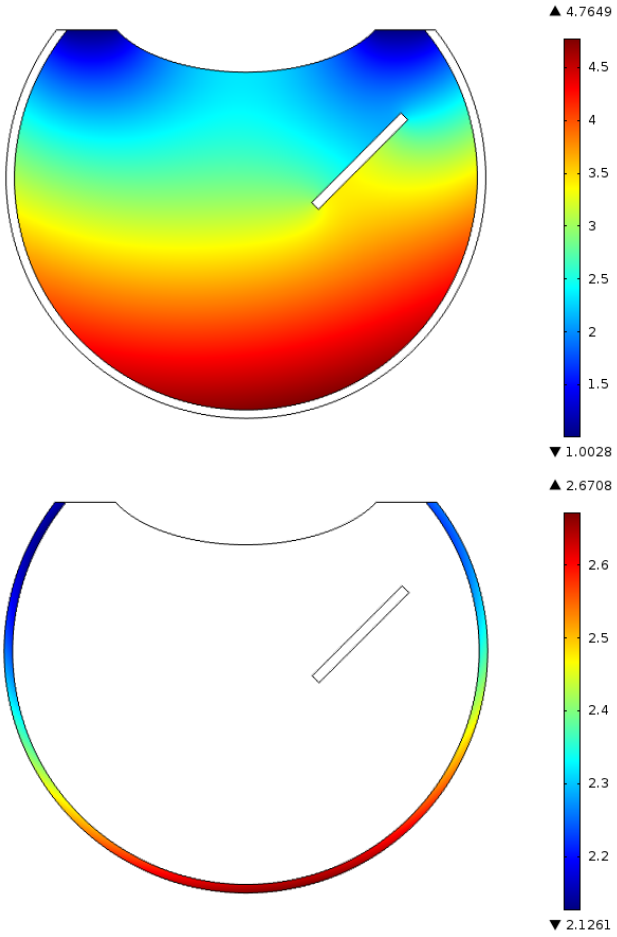

Figure 6: Distribution of drug concentration after 4 months of release in the vitreous (up) and retina (down).

In Figure 6 we plot the drug concentration in the vitreous chamber and in the retina after 4 months of drug release. On the top we observe that the drug accumulates near $\partial\Omega_{2,3}$, adjacently to the retina. This pattern suggests a convection dominated transport. Even if the continuity of concentration is not used in the boundary interface $\partial\Omega_{2,3}$, a similar pattern of drug distribution is observed in the retina. In the bottom plot of Figure 6 we can observe that the drug concentration is higher in the region of the optic nerve (Figure 1).

Liquefied vitreous: influence on the velocity

The question of until what extent the liquefaction will affect drug distribution in the retina is now addressed. We will study its influence though the velocity of the flow in the vitreous.

The heterogeneity of the vitreous is represented geometrically by two regions with a larger permeability (20 times larger than in the non liquefied part)(Figure 7). This scenario corresponds to an early state of vitreous liquefaction where lacunae haven't yet occurred. In Figure 7 we plot the velocity of the fluid in the vitreous. Comparing the scales of the velocity fields in Figure 5 and Figure 7 we observe that slightly lower velocities occur in Figure 5.

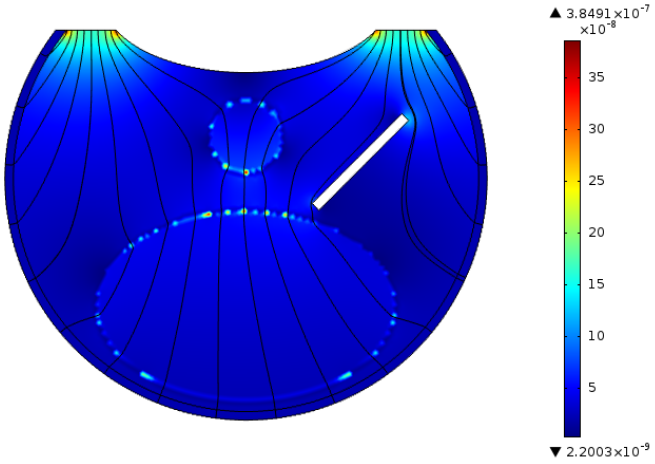

Figure 7: Velocity in the vitreous when a liquefaction occurs.

However the velocities in the case of liquefaction are of the same order of magnitude as in the case it is assumed that no liquefaction occurs. In a certain sense this is an expected result and is in agreement with previous studies ([20]). In fact from the calculated steady state pressure (Figure 5), we concluded that the vitreous accounts for 1.25% pressure drop. This means that the volumetric flow rate can not rise more than by 1.25% even if the permeability of the vitreous becomes very high. Consequently, the average velocity will stay in the same order of magnitude after the vitreous liquefaction.

In Figure 8 we compare drug concentration during 4 months of release in these two different situations: normal vitreous (N. Vitreous) and early liquefied vitreous (Liq. Vitreous). These results suggests a relative unimportance of the vitreous liquefaction for the drug distribution if only the influence of vitreous permeability on velocity is considered. However the increase of permeability of the vitreous could facilitate the movement of the implant, or even alter the partition coefficient A_2, between vitreous and retina. The dependence of drug release on the position of the implant is addressed in what follows.

Position of the implant

To analyse the influence of liquefaction on the drug distribution, when a movement of the implant occurs, we solve for a new position of the implant the previous problem.

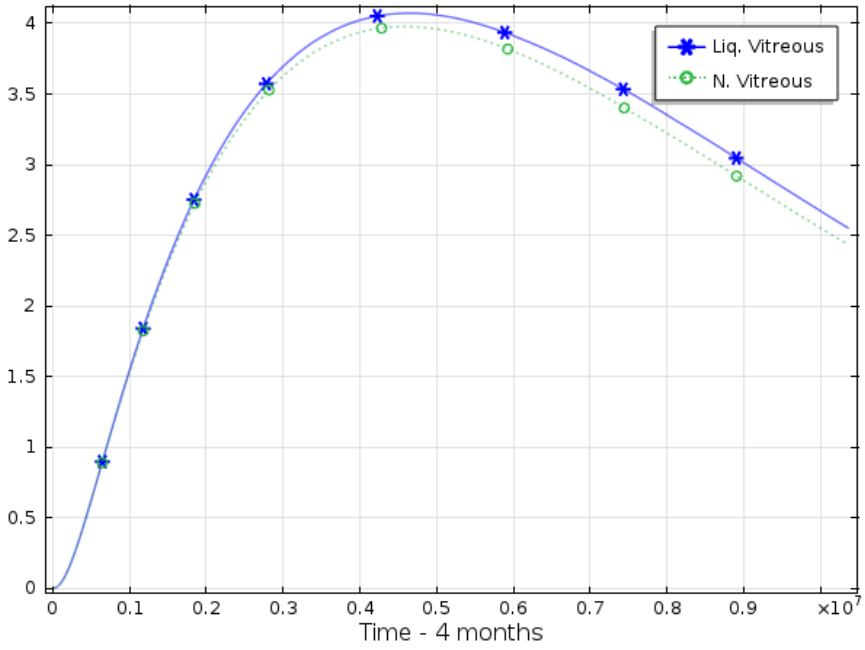

Figure 8: Mean drug concentration in the retina during 4 months: in the case of a normal vitreous (N. Vitreous) and of a liquefied vitreous (Liq. Vitreous).

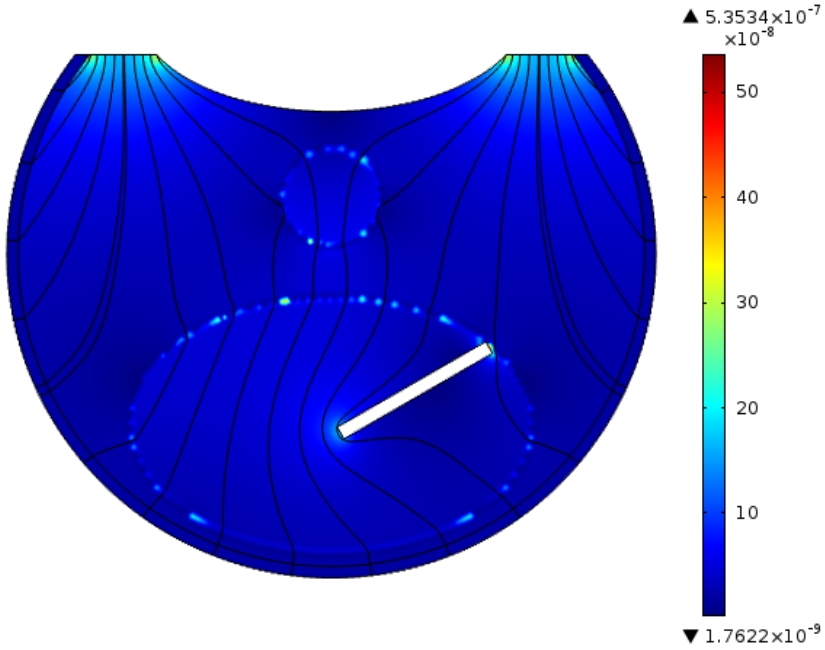

Figure 9: Velocity in the vitreous with an early liquefaction in a new position of the implant(Po_2).

We present in Figure 9 a two dimensional plot of the velocities. We conclude that for the new position of the implant the velocities are aproximately of the same order of magnitude.

Let us represent by Po_1 the position of the implante in Figure 7 and by Po_2 the position of the implant in Figure 9. The question to be answered is then the following: can vitreous liquefaction influence drug distribution in the retina, through the occurrence of movement of the implant? For the two positions described before the answer is negative as exhibited in Figure 10 because the difference in the mean concentration in the retina is not meaningful.

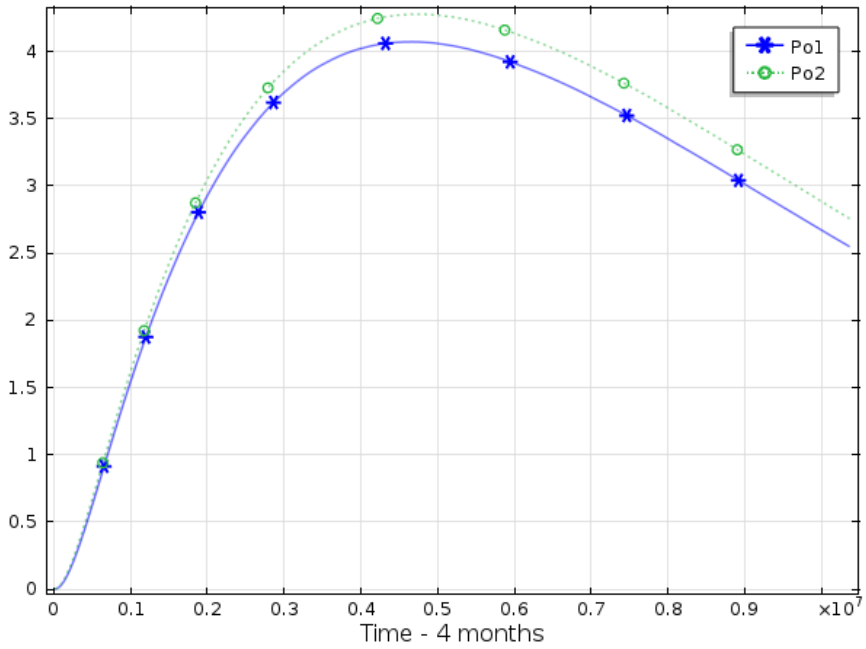

Figure 10: Mean concentration of drug in the retina during 4 months: in the case of position Po_1 and position Po_2.

3.2 Blood Retinal Barriers

The Blood Retinal Barrier (BRB) prohibits the passage of macromolecules and other cells from the blood vessels to the intraretinal compartment. It is composed by the inner blood retinal barrier (iBRB) and the outer blood retinal barrier (Figure 11).

Some ocular pathologies are accompanied by the breakdown of theses barriers, that have a direct implication on the pharmacokinetics of drugs. The breakdown of the barriers is mathematically described by a decrease of A_2 and A_3.

Dependence on the parameters A_2 and A_3

In the framework of our model A_2 represents the partition coefficient of the interface vitreous-retina, that is the iBRB, and A_3 is a key parameter to represent the retinal clearance.

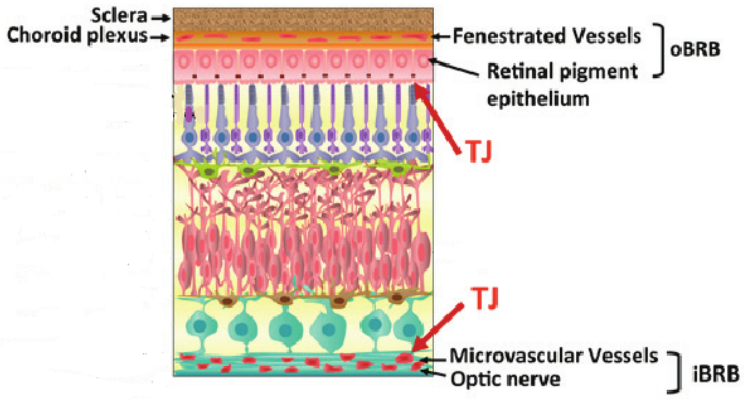

Figure 11: Blood Retina Barriers - Adapted from Figure 5 of $TightJunctions(2012)DOI$: 10.5772/35166 *Current Frontiers and Perspectives in Cell Biology*

We illustrate in Figures 12 and 13 the dependence of the mean drug concentration on these parameters. As reported in [9] "Diabetic Retinopathy is initiated by an alteration of the iBRB and Age Macular Degeneration is a result of an alteration of the outer BRB. Macular edema is a direct result of alterations of the BRB."

In Figure 12 we represent the evolution of drug mean concentration in the retina for an initial stage of diabetic retinopathy. As the diseases progresses the peak and the residence time decrease.

In Figure 13 we illustrate the dependence of the drug mean concentration in the retina on the initial stage of age macular degeneration. As the disease progresses the peak and the residence time increase.

We complete the proceeding observations by adding the variation of the retina permeability, K_r. We assume that as inflammation progresses, more edema is observed, which means that narrower are the intercellular paths and less permeable is the retinal tissue. We define two inflammatory scenarios: PI ($A_2 = A_3 = 10^{-9}\,(m/s)$, $\frac{K_r}{\mu_r} = 10^{-10}\ (m^2/(Pa.s))$) and PII($A_2 = A_3 = 4 \times 10^{-9}\,(m/s)$, $\frac{K_r}{\mu_r} = 4 \times 10^{-10}\ (m^2/(Pa.s))$). Retinal process PI represents a more severe condition than PII. We observe that, during the initial uptake, a higher concentration is observed in the retina in PII. The peak in PI occurs after 2 months of release. This result is in agreement with [7]. However in a less severe condition as PII the peak occurs after one month of release. These results suggest that as disease in retina progresses, the concentration peak and the residence time increase.

Effect of a successful treatment

It is expected that as the drug penetrates the retina a therapeutic effect is felt, increasing A_2 and A_3. We conclude this subsection by illustrating the influence on drug concentration

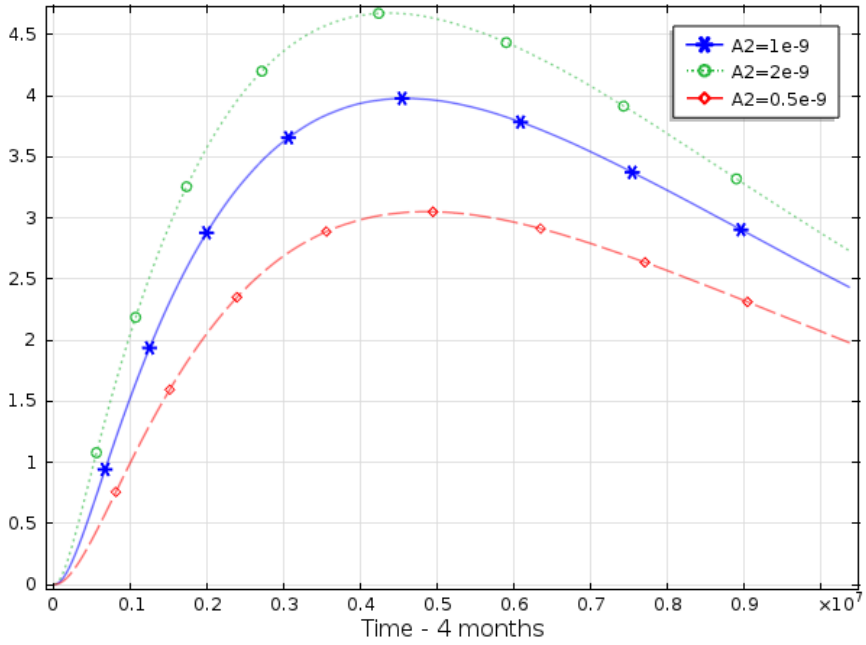

Figure 12: Influence of A_2 in the mean concentration of drug in the retina during 4 months.

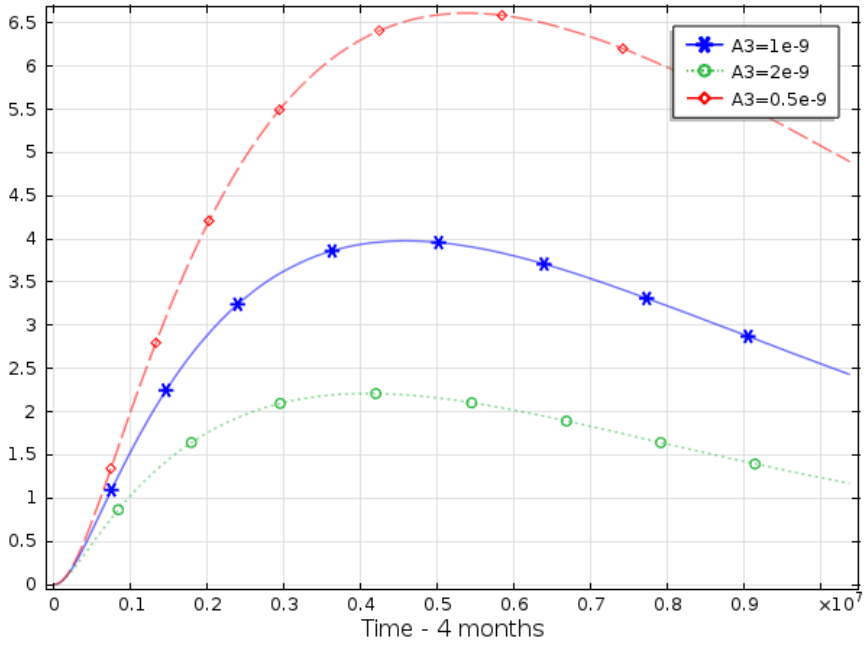

Figure 13: Influence of A_3 in the mean concentration of drug in the retina during 4 months.

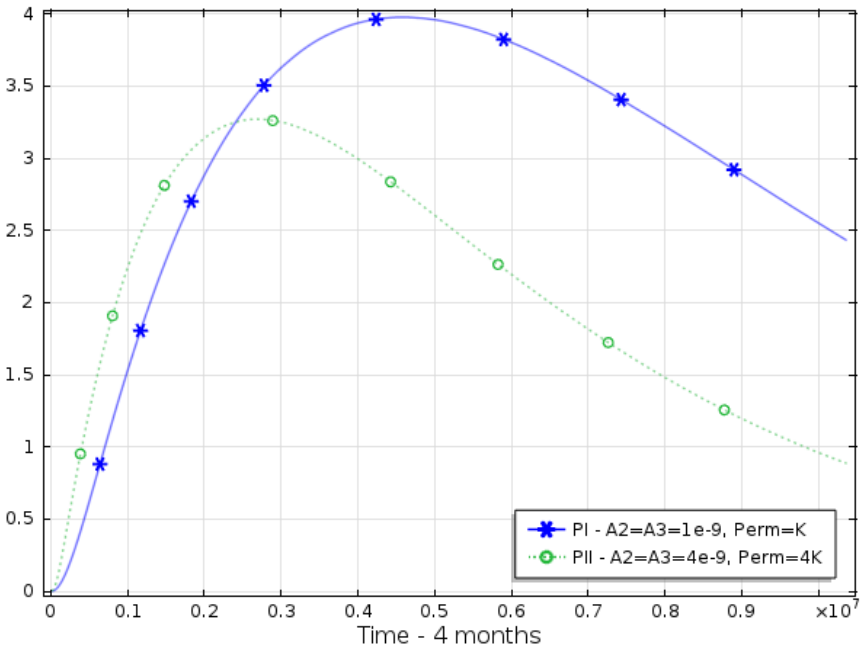

Figure 14: Influence of retina diseases in the mean concentration of drug in the retina during 4 months.

in the retina of a time evolving A_3. We assume a constant A_2. We begin by considering a normal IOP ($2000Pa$) and a normal fluid pressure in the choroid ($P_{out} = 1200Pa$).

In Figure 15 we exhibit a possible representation of A_3 as a function of time, under the action of the drug. The plot of A_3, which has an academic character, has been obtained by interpolation, using piecewise cubic functions and assuming that a significant change in the retina, due to the therapeutic effect of the drug, is observed each 15 days.

In Figure 16 we exhibit a plot of the drug concentration in the retina, when A_3 is defined by the function in Figure 15. The plot in Figure 16 suggests that the model is very sensitive to A_3. As the drug acts then A_3 increases and the peak and the residence time are smaller than it could be expected with a constant A_3.

We can now ask if the success of the treatment depends on the IOP and the choroid fluid pressure, P_{out}, on the boundary $\partial\Omega_{out}$. We illustrate in Figure 17 the influence of IOP on the drug mean concentration in the retina. The results suggest that as the IOP increases, higher is the peak of drug concentration in the retina.

Regarding the pressure P_{out}, Figure 18 suggests that higher is the blood pressure, smaller is the peak but larger is the residence time.

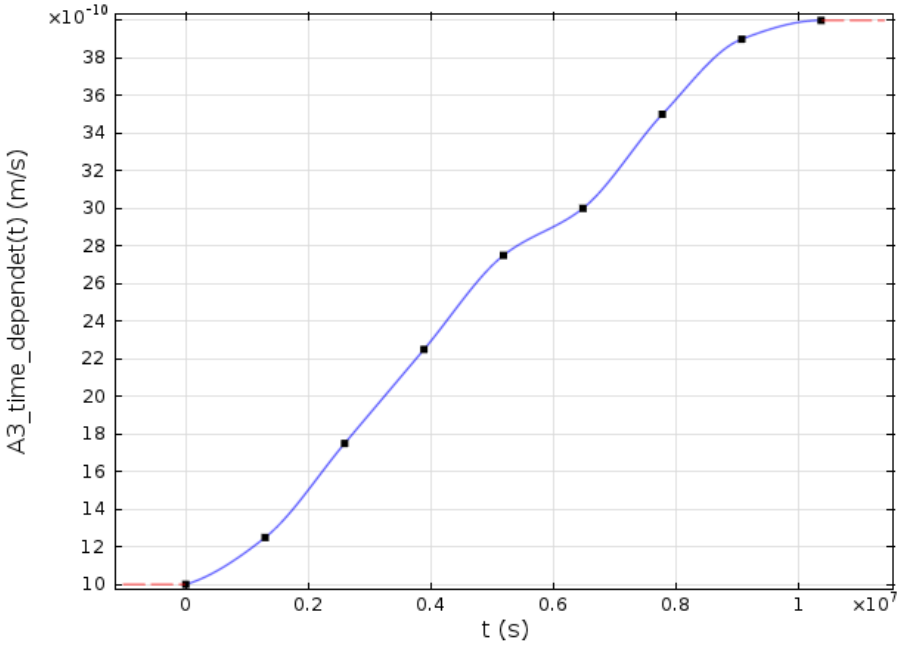

Figure 15: Ansatz for a plot of A_3 as a function of time during 4 months.

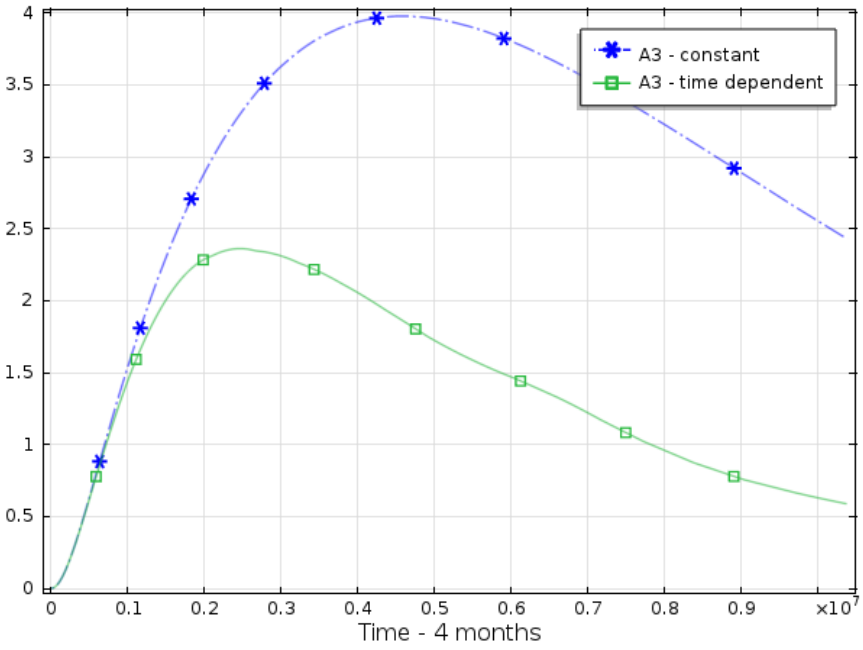

Figure 16: Influence of an evolving A_3 on the mean concentration of drug ($A_3 = 1 \times 10^{-9}$ or as a time dependent function).

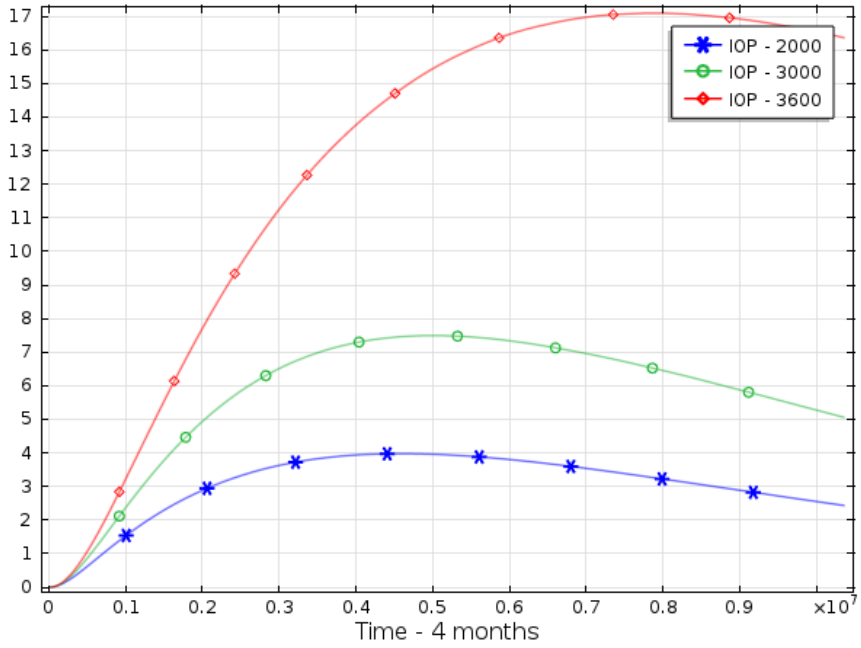

Figure 17: Influence of IOP in the mean concentration of drug in the retina during 4 months for $P_{out} = 1200$.

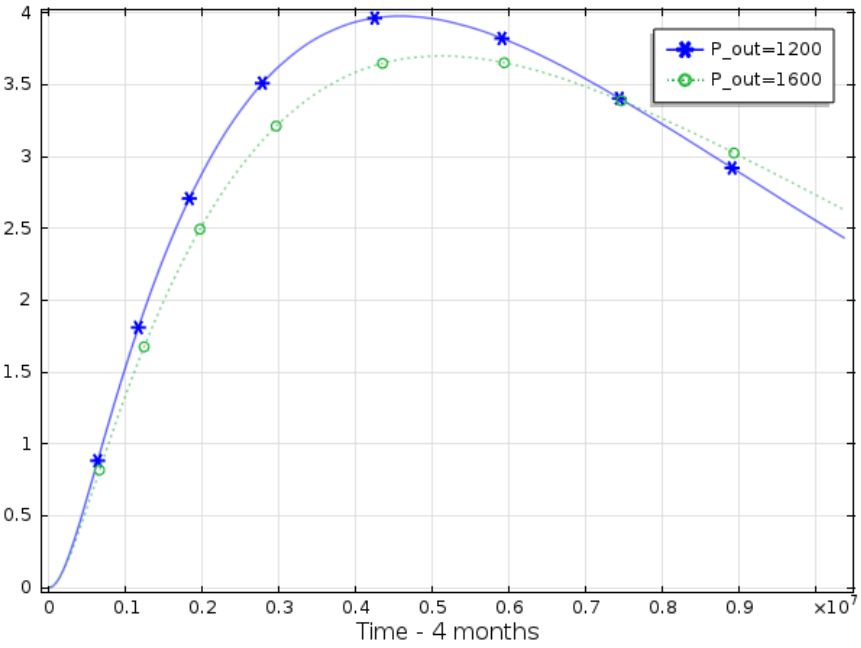

Figure 18: Influence of P_{out} in the mean concentration of drug in the retina during 4 months with $IOP = 2000$.

4 Final Comments

The aim of this paper is to answer the following question: what are the main differences in the pharmacokinetics of a drug in case of anomalies of the vitreous humor, due to aging as liquefaction, and retina diseases? Two cases are analysed: liquefaction of the vitreous humor and decreased clearance of the retina due to different pathologies.

Our main conclusions are summarized in what follows:

(i) Liquefaction of the vitreous

The peak and residence time of the drug concentration in the retina are not very sensitive to the degree of liquefaction of the vitreous (Figure 7).

The peak and residence time of drug concentration in the retina are just slightly sensitive to the movement of the implant that can be induced by the vitreous liquefaction (Figure 10).

(ii) Retinal Clearance

The peak and residence time of the drug concentration in the retina is very sensitive to partition coefficient vitreous-retina A_2 and the rate of clearance A_3 (Figures 12 and 13). Meaningful differences can be observed in the first stages of diabetic retinopathy and age macular edema.

(iii) Intraocular pressure In case of high intraocular pressure higher concentrations peaks are observed in the retina(Fig 16).

If the ocular globe moves smoothly or doesn't move at all our simulations suggest that the aging of vitreous, under the form of liquefaction, doesn't have a meaningful influence, in the concentrations plots in the retina. In future work saccade movements will be addressed. On the contrary our studies suggest that the influence of the tight junctions of the retinal epithelium - which opening means a breakdown of the blood retinal barrier and consequently a decrease in the clearance - is determinant in predicting peak and residence time.

Acknowledgements

This work was partially supported by the Center for Mathematics of the University of Coimbra - UID/MAT/00324/2013, funded by Portuguese Government through FCT/MEC and co-funded by through the Partnership Agreement PT 2020.

A Annex

Symbol	Definition (unities)
C_1	drug concentration in the implant (mol/m^3)
C_2	drug concentration in the vitreous (mol/m^3)
C_3	drug concentration in the retina (mol/m^3)
M	polymer molecular weight $(Dalton)$
D_0	diffusion coefficient (m^2/s)
D_1	diffusion function depending on M (m^2/s)
D_2	diffusion coefficient of drug in the retina and vitreous (m^2/s)
M_0	initial molecular weight in the implant
C_0	initial drug concentration in the implant (mol/m^3)
p	pressure (Pa)
v_2	velocity of the aqueous humor in the vitreous (m/s)
v_3	velocity of the aqueous humor in the retina (m/s)
K	permeability of the vitreous (m^2)
μ_1	viscosity of the permeating aqueous humour $(Pa.s)$
ρ	density of water (Kg/m^3)
A_1	partition coefficient of the interface implant-vitreous (m/s)
A_2	partition coefficient of the interface vitreous-retina (m/s)
A_3	retinal clearance (m/s)
$\overline{k}$	degradation rate $(1/s)$
β_1, β_2	degradation rate of the polymer $(1/s, Dam^3/(mol.s))$
K_r	permeability of the retina (m^2)
μ_r	viscosity of the aqueous humor in the retina $(Pa.s)$
$\frac{K_r}{\mu_r}$	hydraulic conductivity of the retina $(m^2/(Pa.s))$

References

[1] M. A. Akhmanovaa, S. P. Domogatskyb, V. Yu. Evgrafovc, Computer simulation of hydraulic flows in the human eye, Biophysics, 56 (2011) 108-113.

[2] E. Azhdari, J.A. Ferreira, P. de Oliveira, P.M. da Silva, Diffusion, viscoelasticity and erosion: analytical study and medical applications, Journal of Computational and Applied Mathematics, 275 (2015) 489-501.

[3] E. Azhdari, J.A. Ferreira, P. de Oliveira, P.M. da Silva, Numerical and analytical study of drug release from a biodegradable viscoelastic platform, Mathematical Methods in Applied Sciences, (2015), DOI: 10.1002/mma.3375.

[4] R.K. Balachandran, V.H. Barocas, Computer modeling of drug delivery to the posterior eye: effect of active transport and loss to choroidal blood flow, Pharmaceutical Research 25 (2008) 2685-2696.

[5] R.K. Balachandran, V.H. Barocas, Finite element modeling of drug distribution in the vitreous humor of the rabbit eye, Annals of Biomedical Engineering 25 (1997) 303-314.

[6] K. A. Barton, Y.B. Shui, J. M. Petrash, D. C. Beebe, Comment on: the Stokes-Einstein equation and the physiological effects of vitreous surgery. Acta Ophthalmologica Scandinavica, 85 (2007) 339-340.

[7] A. Chan, L.S. Leung, M.S. Blumenkranz, Critical appraisal of the clinical utility of the dexamethasone intravitreal implant (Ozurdex) for the treatment of macular edema related to branch retinal vein occlusion or central retinal vein occlusion, Clin Ophthalmol, 5 (2011) 1043-1049.

[8] J.E. Chang-Lin, J.A. Burke, Q. Peng, et al., Pharmacokinetics of a sustained-release dexamethasone intravitreal implant in vitrectomized and nonvitrectomized eyes. Investigative Ophthalmology and Visual Science., 53 (2011) 4605–4609.

[9] J. Cunha Vaz, R. Bernardes, C. Lobo, Blood-Retinal Barruier, European Journal of Ophthalmology, 21 (2011).

[10] V. Delplace, S. Payne, M. Shoichet, Delivery strategies for treatment of age-related ocular diseases: From a biological understanding to biomaterial solutions, Journal of Controlled Release 219 (2015) 652-668.

[11] H.F. Edelhauser, C.L. Rowe-Rendleman, M.R. Robinson,3 D.G. Dawson, G.J. Chader, H.E. Grossniklaus, K.D. Rittenhouse, C.G. Wilson, D.A. Weber, B.D. Kuppermann, K.G. Csaky, T.W. Olsen, U.B. Kompella, V.M. Holers, G.S. Hageman, B.C. Gilger,P.A. Campochiaro, S.M. Whitcup, W.T. Wong, Ophthalmic Drug Delivery Systems for the Treatment of Retinal Diseases: Basic Research to Clinical Applications, Investigative Ophthalmology and Visual Science, 51 (2010) 5403-5420.

[12] C.R. Ethier, M. Johnson, J. Ruberti (2004), Ocular Biomechanics and Biotransport, Annual Review of Biomedical Engineering, 6 (2004) 249-273.

[13] J.A. Ferreira, P. de Oliveira, P.M. da Silva, R. Silva, A mathematical model of controlled drug release in a completely detached vitreous, Proceedings of the 15th International Conference on Computational and Mathematical Methods in Science and Engineering, CMMSE 2015, (2015) 508-519.

[14] N.G. Ghazi, W.R. Green, Pathology and pathogenesis of retinal detachment, Procedings of Cambridge Ophthalmological Symposium Eye, 2002.

[15] U.H.E. Grossniklaus, J.M. Nickerson, H.F. Edelhauser, L.A.M.K. Bergman, L. Berglin , Anatomic Alterations in Aging and Age-Related Diseases of the Eye. Investigative Ophthalmology and Visual Science, 54 (2013).

[16] N. Haghjou, M.J. Abdekhodaie, Y.L. Cheng. M. Saadatmand, Computer modeling of drug distribution after intravitreal administration, W.A.S. Engineering and Tecnology 53 (2011) 706-716.

[17] Jing Xu, J.J. Heys, V.H. Barocas, T.W. Randolph, Permeability and diffusion in vitreous humor: implications for drug delivery, Pharmaceutical Research, 17 (2000) 664-669.

[18] J. Kathawate, S. Acharya, Computational modeling of intravitreal drug delivery in the vitreous chamber with different vitreous substitutes, International Journal of Heat and Mass Transfer 51 (2008) 5598–5609.

[19] L.L. Lao, S.S. Venkatraman, N.A. Peppas, Modeling of drug release from biodegradable polymer blends, European Journal of Pharmaceutics and Biopharmaceutics 70 (2008) 796–803.

[20] T,U,V,Y.T, Lay Ean Tan, A model of ageing vitreous: implications for drug delivery, PhD Thesis, University of Glasgow, 2010.

[21] S.J. Ryan, A.P. Schachat, C.P. Wilkinson, D.R. Hinton, S.R. Sadda, Retina, 5th Edition, 2012.

[22] S. Rothstein, W.Federspiel, S. Little, A unified mathematical model for the prediction of controlled release from surface and bulk eroding polymer matrices, Biomaterials 30 (2009) 1657–1664.

[23] A.R.H. Simpson, R. Petrarca, T. L. Jackson, Vitreomacular adhesion and neovascular age-related macular degeneration, Survery of Ophthalmology, 57 (2012) 498-509.

[24] M.S. Stay, J. Xu, T.W. Randolph, V.H. Barocas, Computer simulation of convective and diffusive transport of controlled-release drug in the vitreous humor, Pharmaceutical Research, 20 (2003) 96-102.

[25] Stefánsson E, Loftsson T, The Stokes-Einstein equation and the physiological effects of vitreous surgery, Acta Ophthalmologica Scandinavica, 84(6), (2006) 718-719.

[26] L.E. Tan, W. Orilla, P.M. Hughes, S. Tsai, J.A. Burke, C.G. Wilson, Effects of vitreous liquefaction on the intravitreal distribution of sodium fluorescein, fluorescein dextran, and fluorescent microparticles, Investigative Ophthalmology and Visual Science, 52 (2011) 1111-1118.

[27] T. Yasukawa, Y. Ogura, H. Kimura, E. Sakurai, Y. Tabata, Drug delivery from ocular implants, Expert Opin Drug Deliv. 3 (2006) 261–273.